Measurement 134 (2019) 762–772

Contents lists available at ScienceDirect

Measurement

journal homepage: www.elsevier.com/locate/measurement

Neutrosophic image segmentation with Dice Coefficients

Sudan Jha [a], Le Hoang Son [b], Raghvendra Kumar [c], Ishaani Priyadarshini [d], Florentin Smarandache [e], Hoang Viet Long [f,g,*]

[a] School of Computer Engineering, KIIT University, India
[b] VNU Information Technology Institute, Vietnam National University, Hanoi, Vietnam
[c] Computer Science and Engineering Department, LNCT College, MP, India
[d] University of Delaware, Newark, DE, USA
[e] Department of Electrical Engineering, University of New Mexico, USA
[f] Division of Computational Mathematics and Engineering, Institute for Computational Science, Ton Duc Thang University, Ho Chi Minh City, Vietnam
[g] Faculty of Mathematics and Statistics, Ton Duc Thang University, Ho Chi Minh City

ARTICLE INFO

Article history:
Received 7 October 2018
Received in revised form 26 October 2018
Accepted 3 November 2018
Available online 10 November 2018

Keywords:
Neutrosophic set
Image processing
Membership and activation functions
Pixel features
Segmentation and augmentation

ABSTRACT

This paper explores various properties of Neutrosophic sets (NS) and proposes a novel idea on Image Segmentation using NS. A theoretical Neutrosophic model is proposed to reduce uncertainty from missing data. Besides, we also tackle the problem of image segmentation with fewer assumptions. Min-Max Normalization is used to reduce any uncertain noise in an image due to a number of factors during image capturing. Next, we apply activation functions to resolve the non-linearity in the image followed by the computed membership functions. These sets are then transformed and compared with others to find similarities and dissimilarities. Neutrosophic Sets and Dice's Coefficients are fused to ensure proper evaluation of uncertainty of the missing data and their indeterminacy for image segmentation. The proposed method is experimentally validated.

1. Introduction

An image incorporates information which is needed to analyze through the process of Image Segmentation. Partitioning of an image into several of these segments (pixels or super-pixels) which is confined to a particular region bound by some characteristics in the forms of texture, intensity or color. If two pixels belong to adjacent regions, their characteristics differ [48]. Therefore, image segmentation is performed in order to locate objects and boundaries. It leads to the assignment of a specific label to each pixel in an image. Regional based segmentation selects a seed pixel and then merges similar pixels around it. Then, there are segmentation techniques based on clustering like K-Means. However, they have their own limitations in the form of overlapping images, computational cost, difficulty in estimating, etc. Hence, more sophisticated methods are used such as image segmentation using fuzzy algorithms, pattern recognition [42] and machine learning [43]. However, these advanced methods have limitations like lack of robustness and variability. Hence, there is a need to present a method of image segmentation that is contemporary and a step ahead. We present neutrosophic image segmentation as a result [47].

Neutrosophic science incorporates neutrosophic logic (NL) and its applications in many fields. It is conceivable to characterize the neutrosophic measure (NM), neutrosophic integral (NI), neutrosophic probability (NP) in light of the fact that there are different kinds of indeterminacies we have to highlight [50–54]. NM is a speculation of the established measure for the situation where the space containing some indeterminacy whereas NP is a speculation of the established and uncertain probabilities. A few traditional probability rules are balanced as NP rules. Moreover, they can be shown by different particular methodologies along with

Abbreviations: NS, Neutrosophic Sets; D_{Score}, Dice's Coefficients; NL, Neutrosophic Logic; NM, Neutrosophic Measure; NI, Neutrosophic Integral; NP, Neutrosophic Probability; FS, Fuzzy Set; IFS, Intuitionistic Fuzzy Set; RS, Rough Set; INS, Interval Valued NS; GPU, Graphics processing units; ABC, Artificial Bee Colony; FDB, Factorized Directional Bandpass; NSC, Neutrosophic Similarity Clustering; SVM, Support vector machine; FOM, Figure of Merit; ROC, Receiver operating characteristic; T, E, C, R, P, D, t, I, f, F, X, Threshold based, Edge-based, Cluster-based, Region-based, PDE-based, Deep-learning based, truth, numerical indeterminacy, falsehood, falsehood membership function, universe of discourse; SNS, Soft Neutrosophic Sets.

* Corresponding author at: Division of Computational Mathematics and Engineering, Institute for Computational Science, Ton Duc Thang University, Ho Chi Minh City, Vietnam; Faculty of Mathematics and Statistics, Ton Duc Thang University, Ho Chi Minh City, Vietnam.

E-mail addresses: jhasudan@hotmail.com (S. Jha), sonlh@vnu.edu.vn (L.H. Son), raghvendraagrawal7@gmail.com (R. Kumar), ishaani@udel.edu (I. Priyadarshini), smarand@unm.edu (F. Smarandache), hoangvietlong@tdtu.edu.vn (H.V. Long).

https://doi.org/10.1016/j.measurement.2018.11.006
0263-2241/

the likelihood theory, fuzzy set (FS) [1], rough set (RS) [2], intuitionistic fuzzy set (IFS) [3], and neutrosophic set (NS) [3]. Molodtsov [4] successfully proposed a novel delicate set theory by utilizing traditional sets since it has been brought up that delicate sets are not appropriate to manage dubious and fuzzy parameters. IFSs can just deal with inadequate data in light of the fact that the whole of degree genuine, indeterminacy and false is one in IFSs. However, NSs can deal with the uncertain and contrasting data which exist regularly in conviction frameworks in NS since indeterminacy is evaluated with free truth-membership, indeterminacy-membership and lie membership [5]. NSs can handle inadequate data, yet not the uncertain and contrasting data which exist normally in genuine circumstances. Several other related research papers featured neutrosophic science [49,50]. Broumi and Smarandache [6] presented the idea of correlation coefficients of interval valued NS (INS). Solis and Panoutsos [7] exhibited another system for making Granular Computing, Neural-Fuzzy displaying structures by means of Neutrosophic Logic to sort-out the problem of vulnerability amid the information granulation process.

The previous works focused on specific characteristics like texture, intensity or color. However, they have limitations in the form of overlapping images, computational cost, difficulty in estimating, etc. Hence, we use Dice's Coefficients (DScore) to resolve earlier sophisticated methods and to ensure proper evaluation of uncertainty of the missing data for image segmentation. Specifically, we propose new definitions regarding various features of an image using membership functions, activating them and then applying fitness functions. A universe of discourse has been defined, and subsequently the subsets are used with pixels as the most important parameters. We use fuzzy set partially and neutrosophic set along with rigorous mathematical operations on real numbers with real standard subsets. They involve crisping an image into smaller non-overlapping subsets so that the characteristics of the image can be explored at a molecular level for better analysis. Mathematical modeling is done for better accuracy for identifying an object. This is our contribution in this paper.

The rest of the paper is organized as follows: Section 2 presents the background of the paper. Section 3 shows the proposed method. Sections 4 and 5 give experiments and conclusions.

2. Literature review

In this section, we list out a few of the existing works that target the process of image segmentation. Taha and Hanbury [31] proposed an efficient evaluation tool for 3D medical image segmentation. Some of the metrics considered for this research are sensitivity, specificity, rand index, Jaccard index, average distance, probabilistic distance, etc. Thai et al. [32] presented a filter design and performance evaluation for fingerprint image segmentation using the factorized directional bandpass (FDB) segmentation method. A systematic performance comparison was conducted between the FDB method and other fingerprint image segmentation algorithms. For evaluation, the metrics considered are a number of orientations in Angular pass filter, Order of Butterworth bandpass filter, constant for selecting morphology threshold, the number of neighboring blocks, etc. Several aspects of fingerprint image quality may affect segmentation (dryness, ghost fingerprint, small scale noise, image artifacts, scars and creases). Accurate verification may become difficult due to distortions or overlapping of images. Bose and Mali [33] proposed an image segmentation algorithm based on Fuzzy Based Artificial Bee Colony and Fuzzy C means. It takes randomized characters and performs better in terms of convergence, time complexity, robustness and accuracy. The images considered for the research are synthetic, medical and texture images whose segmentation are difficult due to noise and ambiguous. Validity index and time complexity have been used to validate the superiority of the proposed work. The proposed work is well supported by the experimental results, but there could be several limitations of using the Artificial Bee Colony method. It does not take any secondary information and may require new fitness tests on new algorithm parameters. Since it performs a higher number of object evaluations, it may be very slow during sequential processing.

Moftah et al. [34] introduced adaptive k-means clustering algorithm for image segmentation. The idea is to perform image segmentation based on identifying target objects by virtue of optimizations so as to maintain optimum results during iterations. It is an extension to the traditional k-means clustering algorithm so as to increase effectiveness and efficiency. The experimental results exhibit the overall performance of the adaptive clustering algorithm in terms of entropy, standard deviation, mean, circularity, orientation and solidity. The major drawback is the fact that there were three samples considered, out of which for only one sample the proposed algorithm showed significant increase. For the other two samples, there was not much improvement. Liu et al. [35] presented a modified particle swarm optimization technique for image segmentation. The aim is to address the issue of computational expense by applying strategies to improve the performance of the initial particle swarm optimization technique. 16 standard test images have been considered in the experimental analysis, which validated that the modified technique is much more superior than the original method in terms of performance and quality. The parameters considered are twelve benchmark functions like quadric, rosenbrock, step, quadric noise, ratrigin, noncontinuous restrain, etc. The issue with the proposed method is the small dataset an only 30 independent runs that have been considered for validating the research, which questions the robustness and application in real world scenarios.

Ayyoub et al. [36] proposed a GPU based implementation of the fuzzy C-means algorithm for image segmentation to address the issue of large data set and slow processing. The idea is to introduce a parallel processing unit to validate the same. A faster variant of fuzzy-c means has been implemented on different GPU cards i.e., Tesla M2070 and Tesla K20m. Experimental analysis reveals that the proposed technique is significantly fast. Speed up, execution time, performance and memory are some parameters which validate the experimental analysis. Due to parallel processing, the process may be computationally expensive. Kloster et al. [37] suggested an image segmentation and outline feature extraction tool for microscopic analysis. The tool SHERPA (SHapE Recognition, Processing and Analysis) could identify and measure objects, and incorporate functions like object identification and feature extraction. It could also perform full image analysis, multiple segmentation methods, matching an object against templates, object scoring and processing large batch of images. Several parameters were taken into consideration for the same, some of which are area, parameter, width, height, optimization method, standard deviation, ellipticity, roundness, compactness etc. The issue with the proposed technique is that it cannot deal with texture and structural features; thereby questioning its versatility and identification specificity.

Chen et al. [38] suggested an interactive image segmentation method in hand gesture recognition so as to recognize the rate of hand gestures effectively. The Gaussian mixture model has been used for image modelling, whereas Gibbs random field is associated with image segmentation and minimization of Gibbs energy for optimal segmentation. The result has been tested on an image dataset and compared with others. The parameters considered are region accuracy and boundary accuracy. Five hand gestures have been relied on for experimental analysis. The limitation of the proposed research work is that it cannot handle issues like highlights, shadows and image distortions. Yu et al. [39] introduced a Semantic Image Segmentation Method with Multiple Adjacency Trees and Multiscale Features. A segment-based classifier and conditional random field are deployed in order to generate large scale regions, whose features have been used for training a region-based classifier. For capturing context, a multiple adjacency tree model has been suggested where each tree denotes a relevant region which can be further generated graphs. Relying on a few assumptions, some inference can be made. MSRC-21 and Stanford background datasets have been used for experimentations. The accuracy is determined by Support Vector Machines. The limitation of this research work lies in the assumptions made in order to make inferences. Further, using SVM has its own limitations like slow processing time.

Guo et al. [40] suggested a novel image segmentation approach based on neutrosophic c-means clustering and indeterminacy filtering. The idea is to transfer the image into neutrosophic domain and then the indeterminacy value of the neutrosophic image, devise an indeterminacy filter. Neutrosophic c-means clustering then clusters the pixels into several groups to find intensity. After the indeterminacy filtering operation, segmentation results are produced. The neutrosophic similarity clustering (NSC) segmentation algorithm has been compared to the proposed method quantitatively. Signal to noise ratio and misclassification error measure are some parameters considered for this research. Figure of Merit (FOM) has been used to measure the difference between the real results with the ideal segmentation result and the difference is not significant. Other works can be found in [23–29,41,46,55–67].

3. Methodology

3.1. Ideas

A universe of discourse is defined, and subsequently the subsets have been used using pixels as the pixels are the most important parameters for any image segmentation. We use Neutrosophic set along with DS_{core} with rigorous mathematical operations on real numbers with real standard subsets. It involves crisping an image into smaller non-overlapping subsets for better analysis. A new definition of DS_{core} is shown as:

$$D_{score} = \frac{S \cap T}{S \cup T}$$

where S is the area of segmentation of the object using our method and T is the manual or original area of segmentation of the object or the ground truth value. To calculate DS_{core}, we have assumed the following parameters which are applicable to all images:

Threshold based = "T",
Edge-based = "E",
Cluster-based = "C",
Region-based = "R",
PDE-based = "P",
Deep-learning based = "D".

Here the (t, I, f) -NS is referred as t = truth, I = numerical indeterminacy, f = falsehood. The (t, I, f) [3] are non-identical from the Neutrosophic Algebraic Structures (NAS) defined in the form of A + bI, where I = literal Indeterminacy. We render the image as I-NAS i.e., this is an algebraic structure established on indeterminacy "I" only. However, we can merge them and get the (t, I, f) -INAS. This means that the algebraic structures based on Neutrosophic Ontology (NoU) in the form a + bI where a and b are the real numbers, a is the determinant part on N, bI is the in-determinant part of N, bI $\subseteq$ mI + nI = (m + n) I, 0•I = 0, I^n = I for integer $n \geq 1$, I/I = undefined. When a, b are real numbers, then a + bI gives real numbers as results. If at least one of a, b is a complex number, then a + bI is known as a N complex number. These structures, in any field of learning, are considered from a NL perspective, i.e., from the truth-indeterminacy-falsehood (t, i, f) values [7,25,27,28].

3.2. Support Neutrosophic set (SNS)

Let X be a nonempty set, where $x \in X$, called the universe of discourse. First, let us define some terms about fuzzy set and Neutrosophic set. Here, we use mathematical operations on real numbers. Let A1 and A2 be two real standard or non-standard subsets, then we can apply some basic set operations such as [8–24]:

$$A1 + A2 = \{x|x = a1 + a2, a1 \in A1, a2 \in A2\}$$

$$A1 - A2 = \{x|x = a1 - a2, a1 \in A1, a2 \in A2\}$$

Now, we perform complementary operations and compute the Cross Product of the two sets, A1 and A2:

$$A2^{-} = \{1^{+}\} - A2 = \{x|x = 1 - a2, a2 \in A2\}$$

$$A1 \times A2 = \{x|x = a1 \times a2, a1 \in A1, a2 \in A2\}$$

Given a subset Y of a partially ordered set X, the Infimum, represented as in (Y), is the is greatest element in X, that is, X ({all elements in Y}, Conversely, The Suprema of Z on a partially ordered set X, represented as sup (Z), is the smallest element in X that is, X ({all elements in Z}, Therefore, we can define the logical operations in terms of Infimum and supreme as follows:

Infimum: A1 $\vee$ A2 = [max {Inf (A1), Inf (A2)}, max {sup (A1), sup (A2)}].

Suprema: A1 $\wedge$ A2 = [min{inf(A1) , inf(A2)} , min{sup(A1) , sup (A2)}].

Observation: Applying Demorgan's Laws, let us consider two cases:

1. If $\inf(A1) \leq \inf(A2)$ and $\sup(A1) \leq \sup(A2)$.

Case 1 above implies that complement of inf(A2) is less than complement of inf(A1) and same for the suprema. From above definitions, we prove that

$$A1 \wedge A2 = A1,\ A1 \vee A2 = A3$$

2. If $\inf(A1) \leq \inf(A2) \leq \sup(A1) \leq \sup(A2)$.

Then, the logical operations can be expressed as the set of infimums and suprema.

Definition 1: A fuzzy set A on the universe X is a function which maps each element in the universe with a truth value $[0,1]^{+}$, also called the degree of membership of an element.

Definition 2: A Neutrosophic set A on the universe X is a function which maps each element with various set membership functions, such as truth membership function T, indeterminacy-membership function I and falsehood membership function F, each representing a truth value. Combining a Neutrosophic set with a fuzzy set leads to a new concept called support-Neutrosophic set (SNS). In which, there are four membership functions of each element in a given set.

Definition 3: A support Neutrosophic set (SNS) in the universe X is a function of four membership functions each corresponding to truth values of either 0 or 1. We denote support Neutrosophic set (SNS) as:

$$A = \{(x, T(x), I(x), F(x), S(x))|x \in X\}.$$

If universe X is continuous then the SNS is the integration of the mapping between each membership function divided by the elements over the entire universe X

$$A = \int < T(x), I(x), F(x), S(x) > /x.$$

If universe X is discrete, then, SNS can be written as the sum of each membership divided by the elements of the universe. If T(x) = I(x) = F(x) = S(x) = 0, *then x is called the worst element.* If T(x) = I(x) = F(x) = S(x) = 1, *then x is called the best element.*

Observations:

1. If the support membership function S(x) attains a constant value c, in a universe of truth labels $[0,1]^+$ then the support Neutrosophic set reduces to a Neutrosophic set.
2. A support-Neutrosophic set is called a standard Neutrosophic set if all the membership functions belong from the set [0,1] and the sum of the functions is less than 1 always.
3. A support-Neutrosophic set is called an intuitionistic fuzzy set if the truth T(x) and falsity FA(x) membership functions belong to [0,1] with their sum less than 1 and the Indeterminacy function I (x) is zero.
4. A constant SNS set can be represented using four symbols having a value between [0,1].

Definition 4: The complement of a SNS set A is denoted by c(A). Here, the truth membership function of c(A) is equal to the Falsity membership function, and vice versa, which is obvious as we are taking the complement of the SNS set. The indeterminacy set of the complementary SNS set is equal to the complement of each element of the original indeterminacy function. The same goes for the support membership function.

Definition 5: A SNS set A is a subset SNS set B if and only if the following conditions are satisfied:

1. The infimum and suprema of T(x) for set A is less than the infimum and suprema of T(x) for set B.
2. The infimum and suprema of F(x) of set A is greater than the infimum and suprema for F(x) of set B.
3. The infimum and suprema of S(x) for set A is less than the infimum and suprema of S(x) of set B.

Definition 6: The intersection of two SNS sets A and B is $D = A \cap B$, defined as follows:

1. The T (x), I (x) and S (x) of D is defined as the corresponding AND functions of the sets A and B.
2. The F (x) of D is defined as the corresponding OR functions of sets A and B.

Example 1: Let U = {x1, x2, x3, x4} be the universe of discourse. Then the support Neutrosophic set A is defined as the sum of all membership functions divided over each element of the universe. Let A = <[0.5,0.8]. [0.4,0.6], [0.2,0.7], [0.7,0.9] >/x1 +...., where, T (x) = [0.5,0.8], I(x) = [0.4,0.6], F (x) = [0.2,0.7] and S (x) = [0.7,0.9]. Then the complement of SNS set A, c (A), is given as c (A) = < [0.2,0.7], [0.4,0.6], [0.5,0.8], [0.1,0.3]>, Here, we see that T(x) of c (A) = F (x) of A, and F (x) of A = T(x) of c (A)

Definition 7 (Distance between support-Neutrosophic sets): Let X = {x1, x2, x3...., x (n)} be the universe set. We define; two support Neutrosophic sets A and B over X which is a universe of discourse.

1. The Hamming distance – It is calculated as the sum of the difference between each corresponding membership function value averaged over all the elements in the universe set.
2. The Euclidean distance – It is calculated as the sum of squares of the difference of the corresponding membership functions averaged over all the elements in the universe U.

3.3. The proposed method

Neutrosophic Sets can be applied on images to acquire understanding on indeterminate and missing data. That is, we are able to apply Neutrosophic sets on missing pixels and still be able to extract information about them. Our method uses activation functions to extract features in a from set of pixels such as edges and circles and then use membership functions to derive useful properties on shades and gradients. A Neutrosophic image I_a can be defined as a set of membership functions, T_s, I_s and F_s. Each image consists of pixel coordinates P (x, y) defined on arbitrary axes. Therefore, each pixel can be assigned membership value with T_s representing the foreground I_s representing the pixel intensity and F_s representing the background or the channels. Given an image I_a, subjected to various kinds of noise, which can be handled by normalization to standardize the pixels. We used non-linear normalization to account for missing and indeterminate data.

$$I(n) = Max(a) - Min(a) * 1/exp\left(1 + \frac{I(a) - \beta}{\alpha}\right) + Min(a) \quad (1)$$

where I (n) is the normalized image with reduced noise, Max (a) and Min (a) are the maximum and minimum pixel intensities in the image, β is the range of pixel intensity values around which image I (a) is centered, α is the width of the input image which is same as the total number of pixels in the image with noise reduction. We apply activation functions to find non-linearity on the segments of the image and found patterns by applying them sequentially on each row. Using Eq. (1), we use a filter size of 2 * 2 with stride 1 and apply a non-linear sigmoid activation function, which serves two purposes:

1. Firstly, it captures shapes such as lines and edges, which are crucial for object detection.
2. Secondly, it squashes each pixel value in the range [0,1] to be used by membership functions. Thus, we apply a non-linear sigmoid activation function *S (z)* as below:

$$S(z) = 1/(1 + exp(-z)) \quad (2)$$

where z is the mean pixel intensity value of the filter which is being activated. From Eq. (2), it is clear that the filters are sets of pixel values based on indeterminacy used to deal with indeterminate and missing data. But for better and smoother segmentation, we used a Gaussian function to smooth out the curves for standardization which is depicted in Eq. (3).

$$G(I(x,y)) = \frac{1}{2\pi\sigma^2} exp\left(-\frac{(x^2 + y^2)}{2\sigma^2}\right) \quad (3)$$

From this equation, we see that

1. If the indeterminacy intensities are low, the variance around the neighborhood is low as well.
2. This results in lowering down the value of σwhich make a less smooth transition around the edges.
3. If σ is large, the current filter neighborhood pixels become smoother.

Therefore, in order to reduce the lowering value of σ, the following equation is used. This is a linear variance function used to transform the filter values to parameter values (Crisping)

$$\sigma = f(I(x,y)) = m * I(x,y) + n \quad (4)$$

where m and n are parameters of the linear function which are used to transform the indeterminacy level to parameter level. A 2×2 filter is a square filter consisting of 4 pixels. We take the mean of these four-pixel values and apply the Gaussian standardization and the activation function. Using the activated values on pixel intensities, we define the truth and indeterminacy membership functionality on the local neighborhood as:

$$T(x,y) = \frac{i(x,y) - i(min)}{i(max) - i(min)} \tag{5}$$

$$I(x,y) = \frac{gd(x,y) - gd(min)}{gd(max) - gd(min)} \tag{6}$$

where I(x,y) corresponds to the intensity of pixel P(x,y) and gd(x,y) corresponds to the gradient magnitude of pixel P(x,y).

Proposed Algorithm: The entire algorithm can be summarized in the following steps:

Step 1: Normalize the Image using Min-Max Method.
Step 2: Apply activation function on successive pixels over the entire image using Gaussian filtering.
Step 3: Find the regions of interest by capturing pixels with higher scores after activation.
Step 4: Compute the membership functions T, I and F by Eqs. ((2), (5), (6)).
Step 5: From the Neutrosophic sets for each object to be identified.
Step 6: Perform De-Neutrosophication and Contrast Reduction to re-construct the objects of interest in the image.
Step 7: Present the results in a Tabular form of fitness scores or values.

The above algorithm can be used for any number of images. For large datasets, we can perform automated using various programs and check the algorithm's accuracy. We can determine the accuracy of our model using Dice's coefficient.

3.4. An illustrative example

In the grayscale image (Fig. 1), it is evident that the background is distorted and not visible. This corresponds to our falsehood membership function to be nearly undefined [30]. The foreground of the image is well defined around the region of the crow, which is the main focus on segmentation. Our goal is to segment each feature such as, the distorted or indeterminate bushes in the background, the features of the crow such as its beak, feathers and its tail, etc. We start by normalizing the image to standardize it and reduce any unnecessary noise in the background. We apply non-linear normalization function in each row and column pixels by using the sigmoid function to transform them to deal with indeterminate pixel values such as the bush near the crow. After normalization, we see that the indeterminacy still prevails, but has improved significantly accordingly with the foreground image. Now, we apply the sigmoid activation functions by taking 2×2 filters to account for the various shapes and edges. We start by applying them from the top-left corner and increment each filter by a stride of 1.

For understanding how this works, we take a small filter segment near the head of the crow. Applying the activation function, near the neighborhood, we find that outside the region of the head, the value of the activation function is significantly low compared to its corresponding filter value after that. We also find that this pattern persists till the end. From this, we can find the edges significantly easier for segmentation.

After applying the activation function, the pixel intensities are squashed between [0,1]. We prepare Neutrosophic sets by defining the truth, indeterminacy and falsehood membership functions. We take each row of the image as a set of Neutrosophics values (Fig. 2). The truth membership function T accounts for the intensity of the pixels in the foreground. We normalize the foreground by using the Min-Max method. In our example, the foreground consists of the crow. The truth membership function defines the patterns in the crow.

The indeterminacy membership function I use the gradients or shades of the neighboring pixels into account (Fig. 3). Therefore, it is a function that defines the lower saturation regions in our image such as the bushes in our example.

The falsehood membership function F operates in the background as opposed to the truth membership function. It would mainly serve by applying the filters on a colored image which has more than one channel. In our image, we have three channels, the falsehood membership function is same as the truth membership function T for each channel. We then define a Neutrosophic set A by combining these three functions for each pixel x in the pixel-space X. Here the universe of discourse X is the set of all pixels in the image, also called as the pixel-space of the image.

$$A = \{(x, T(x), I(x), F(x)) | x \in X\} \tag{7}$$

Now, using this Neutrosophic set, we define a fitness function L, also called Loss function, which will determine the quality of our output generation. This involves the calculation of average Neutrosophic values of each membership function. This analysis shows better insights such as segmentation score etc.

$$L = \left\{ \frac{T(x) + I(x) + F(x)}{3} \right\} \text{ for all } x \in X \tag{8}$$

Fig. 1. Original image to be used for segmentation.

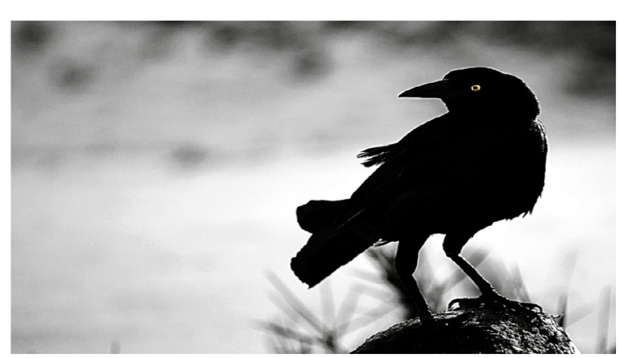

Fig. 2. Truth values after normalization in image.

Fig. 3. Indeterminate values in image.

As we apply the activation functions to downgrade our image, it may look distorted, due to which we need to reconstruct the image for better clarity. Here we use, de-Neutrosophication and contrast reduction to backtrack to a better image clarification. A Neutrosophic set N can be transformed to a de-Neutrosophic set by the following transformation

$$H(x) = \alpha * T(x) + \beta * \frac{F(x)}{4} + \gamma * \frac{I(x)}{2} \tag{9}$$

$$den(H(x)) = \frac{\int_a^b H(x) * xdx}{\int_a^b H(x)dx} \tag{10}$$

Here, $\alpha, \beta and \gamma$ are parameters where $0 \leq \alpha, \beta, \gamma \leq 1$ and $\alpha + \beta + \gamma = 1$, den (H (x)) is the de-Neutrosophic set which is calculated using the center of gravity method. The de-Neutrosophic set consists of the pixel values corresponding to the objects we want to segment. Hence, they can be transformed and compared with other images for better understanding of the model. Let N and M be two Neutrosophic sets, we can find similarities with them using set theory. Using intersect, we can find similarities between two sets.

$$A = N \cap M | T(N) \wedge T(M); I(N) \wedge I(M); F(N) \vee F(M) \tag{11}$$

Using Union, it might be possible to combine two pixel sets as well.

$$B = N \cup M | T(N) \vee T(M); I(N) \vee I(M); F(N) \wedge F(M) \tag{12}$$

Using complement, we can get the negative of an image.

$$C = N \,| T(N) = F_c(N); F(N) = T_c(N); I_c(N) = 1^+ - I(N) \tag{13}$$

We now use the contrast reduction methods from the Eqs. ((11)–(13)) to further clarify the image. We found that by using maximum clarity, the model had accurately identified the object in the frame.

4. Result and discussions

In this section, we focus on extracting the image of the crow [30] to discard other relevant features so that there are no external noises. The Python library OpenCV is a scientific library for solving problems in the computer vision domain. OpenCV takes an image as input and produces an array representing its pixel values as output. The pixel values are in the range (0–255). The original image is converted into its corresponding pixel formats by using OpenCV 2 function imread () converting it to a numpy array. The pseudocode for it can be given as below:

```
Import cv2
im = imread('file.jpg')
The image can be converted to grayscale format
im_gray = cv2.cvtColor(im, cv2.BGR2GRAY)
In order to flip an image vertically, we can use OpenCV flip()
   function which helps us in rotating the image by certain
   degree. The image can be rotated vertically by 180 degrees. The
   pseudocode is given as follows:
im_flip = cv2.flip(im, 1)
The image can be rescaled to a certain degree using OpenCV
   rescale() function. We rescaled the image to 1.5x to better
   analyze our images using the proposed method. The
   followingpseudocode can be used to rescale any image.
r = 1.5 * im.shape[1]
Dim = (100, int(im.shape[0] * r)
resized = cv2.resize(im, dim, interpolation = cv2.INTER_AREA)
```

Firstly, we use normalization to reduce any kind of internal noise. This gives us a better understanding of the objects in the frame, such as the blurred bushes in the background. We use the Min-Max Scaler normalization technique, which is a non-linear normalization process to reduce noise. Let I(X) be the image where X is the pixel-space set or the universe of discourse. Let X = $\{x_1, x_2, x_3 \ldots . x_n\}$ where x_i represents pixels of the flattened image. Then, for the above image we have:

$$N(x(i)) = (255 - 0) * 1/\exp(1 + (x(i) - 1001)/1395) + 0 \tag{16}$$

Using the Min-Max Normalization technique (Fig. 4), it becomes easier to interpret data and reduce noise and other factors which hinder Image processing in general. Therefore, using Normalization is a good start on reducing complexity. For the above image, we get the following normalized image:

We then apply the sigmoid activation function on each Gaussian filter as weights successively on each pixel. Then we compare each output value by the adjacent one. If the adjacent value is less

Fig. 4. Normalized image using non-linear Min-Max Method.

Table 1
Observations of bush, head and tail from original image 1.

Type	Parameters of various types of observations		
Bush	Length (0.23,0.82,0.23)	Width (0.1,0.5,0.1)	Tip (0.02,0.09,0.02)
Head	Break (0.86, 0.78,0.86)	Crown (0.96,0.54,0.96)	Eyes (0.23,0.67,0.23)
Tail	Hand (0.36,0.25,0.36)	Legs (0.24,0.35,0.24)	Fingers (0.48,0.89,0.48)

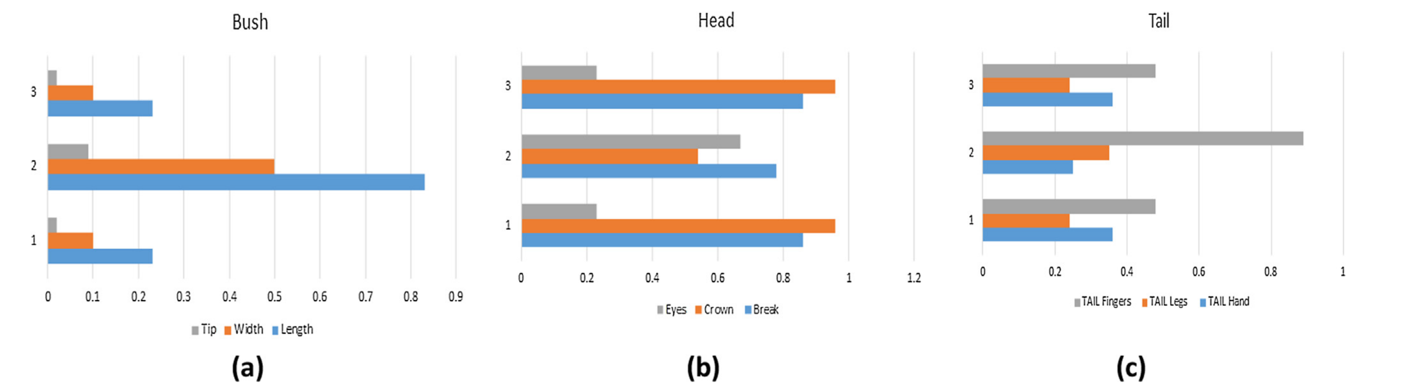

Fig. 5. (a–c): The observational result following Table 2.

Table 2
Observations of bush, head and tail by flipping the original image 1 upside down.

Type	Parameters of various types of observations		
Bush	Length (0.56,0.78,0.0.56)	Width (0.21,0.4,0.21)	Tip (0.07, 0.12,0.07)
Head	Break (0.87, 0.65,0.87)	Crown (0.75,0.65,0.75)	Eyes (0.25,0.78,0.25)
Tail	Hand (0.40,0.89,0.40)	Legs (0.27,0.37,0.27)	Fingers (0.50,0.87,0.50)

Table 3
Observations of bush, head and tail by rescaling the original image by 1.5 × times.

Type	Parameters of various types of observations		
Bush	Length (0.89,0.74,0.0.89)	Width (0.30,0.47,0.30)	Tip (0.89, 0.88,0.89)
Head	Break (0.56, 0.23,0.0.56)	Crown (0.78,0.68,0.78)	Eyes (0.52,0.34,0.52)
Tail	Hand (0.60,0.64,0.60)	Legs (0.67,0.75,0.67)	Fingers (0.50,0.78,0.50)

compared to the next pixel, we start to prepare our Neutrosophic set from the next pixel till the end of the pattern. Given a pixel $x(i) \in X$, the sigmoid activation function is calculated for each Gaussian filter separately.

$$G(I(x,y)) = \frac{1}{2\pi\sigma^2} exp\left(-\frac{(x^2+y^2)}{2\sigma^2}\right) \tag{17}$$

$$S(x(i)) = 1/(1+exp(x(i))) \tag{18}$$

$$R(I(x,y)) = G(I(x,y)) * S(x(i)) \tag{19}$$

Hare, R (I (x, y)) represents the transformed Image after applying the activation function. The Gaussian function keeps track whether the pixels are changing or not. According to those observations, we can pick the pixels which we are interested in and from their corresponding Neutrosophic sets. We form Neutrosophic sets for three sections named, Bush, Head and Tail, each corresponding to the bush, the crow's head, and tail. We then transform the image by rescaling and flipping the image and computing the Neutrosophic values for each transformed image. For the original image, we find the following observations (Table 1):

Referring to Fig. 5(a)–(c), it can be inferred that the orientation of length is in proportion with that of Tip and Width whereas the orientation for Head are almost same. But if we infer to the orientation of Tail, the Tail is highly proportional with respect to Tail Legs and tail Heads (Table 2).

Referring to Fig. 6(a)–(c), it can be inferred that the orientation of length for head is almost consistent whereas the length is highest for "Tail". The reason is due to upside down position of the original image. Likewise, the orientation for Tip gradually increases from Bush to Tail. If we infer to the orientation of Head, it is very clear that the Head is highly proportional with respect to Tail and Bush. We now rescale the image by 1.5 times i.e., the original image × 1.5 times. The observations are tabulated as below (Table 3).

Referring to Fig. 7(a)–(c), it can be inferred that the orientation of Tip, Width and length are almost consistent for all the three i.e., Bush, Head and Tail. Thus, this result infers to the fact that even if we change and rescale our image, the Neutrosophic sets do not

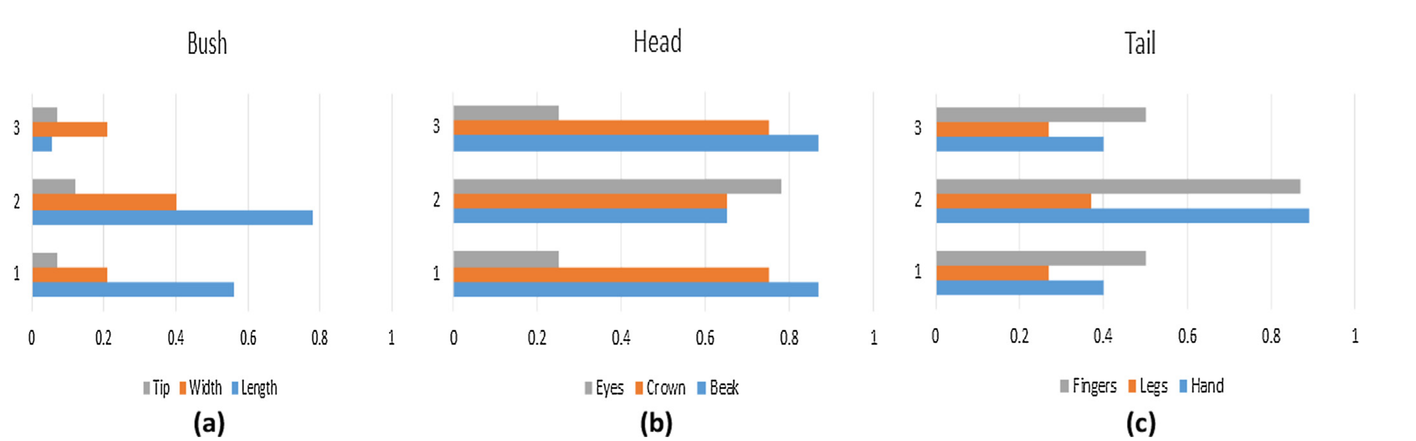

Fig. 6. (a–c): The Observational result following Table 2.

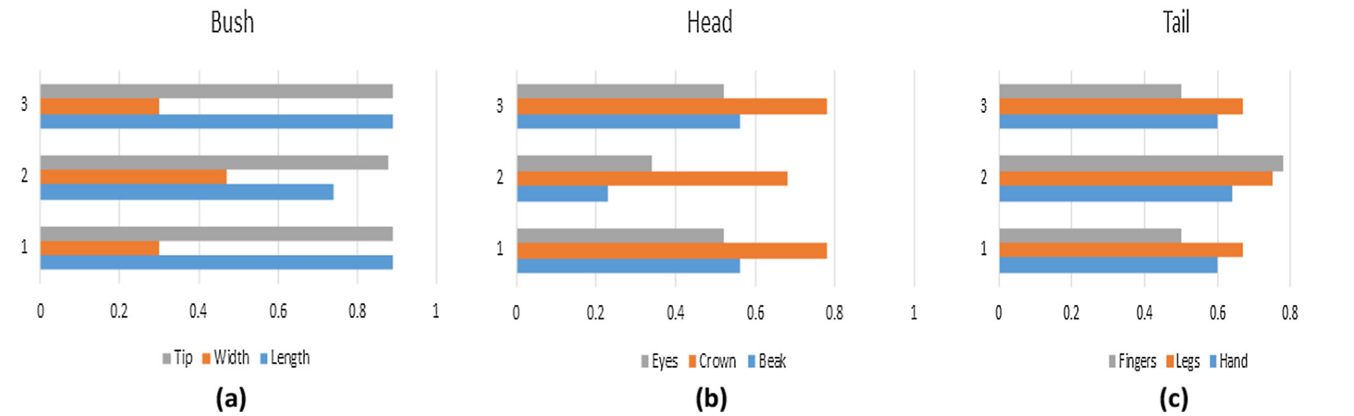

Fig. 7. (a–c): The Observational result following Table 4.

Fig. 8. Final image showing object of interest (crow) in a frame.

Table 4
Comparison for different image orientations using Ds_{core} with neutrosophic sets.

	Parameters of various types of observations taken using the DS_{core}		
Orientation	Bush	Head	Tail
Normal	Length (0.21,0.75,0.19) Width (0.09,0.3,0.03) Tip (0.01, 0.04,0.03)	Beak (0.66,0.68,0.68) Crown (0.86,0.24,0.76) Eyes (0.13,0.37,0.32)	Hand (0.21,0.12,0.13) Legs (0.16,0.23,0.14) Fingers (0.24,0.67,0.29)
Upside Down	Length (0.46,0.38, 0.0.46) Width (0.11,0.3,0.16), Tip (0.04, 0.08,0.04)	Beak (0.75, 0.63,0.76), Crown (0.64,0.46,0.64), Eyes (0.16,0.68,0.15)	Hand (0.31,0.69,0.20), Legs (0.21,0.27,0.19), Fingers (0.43,0.65,0.42)
Rescaling (1.5x)	Length (0.67,0.67, 0.0.71) Width (0.20,0.37,0.21), Tip (0.79, 0.78,0.69)	Beak (0.46, 0.13, 0.0.46), Crown (0.63,0.62,0.65), Eyes (0.42,0.30,0.42)	Hand (0.44,0.44,0.48), Legs (0.61,0.67,0.48), Fingers (0.49,0.65,0.46)

change much, i.e., whatever be the pixel data presented in the same image, the final sets will not alter much. Hence, our observations closely resemble with that of the theoretical observation. Now, the above data can be normalized and cumulatively tabulated as below (Fig. 8).

From the above observations (Table 4), we find that even if we change and rescale our image, the Neutrosophic sets do not change much. This means that however, be the data presented, the final sets will not change much at all and we will get roughly the same results always. This can be proved easily using properties of Neutrosophic sets. Hence, our observations closely resemble the theoretical observations. The below image is the final image after performing all the steps, which shows us the object crow in the frame which is of best interest to us. The comparison between the various segmentation methods with the descriptions as well as advantages and disadvantages are indicated in Table 5.

The Segmentation Method for Threshold based using DS_{core} is observed to be 0.56 whereas using Neutrosophic sets, we obtained 0.78 which is much better accurate value in comparison all other segmentation methods (Table 6).

Now we have shown this analysis with the help of bar graph visualization (Fig. 9).

The proposed method performs better than others as it requires less computation power and time to find the results (Table 7). The results were verified and validated by humans and the method works fine. It is important to note that this method takes very few assumptions about the data provided. The data can be presented with indeterminate form and in different orientations and sizes. The model works on these types of scenarios as well, which makes it unique from other previous works done on Image Segmentation using Neutrosophic sets. In medical diagnosis as an example, most of the data is indeterminate and come in various orientations as well. Sometimes, we need to use sonar projections of certain organs of the body which are captured better at certain

Table 5
Comparison between the various types of image segmentation methods.

Segmentation Methods	Description	Advantages	Disadvantages
Threshold based	Find particular threshold values of the image	No need to hold the previous image related information	Highly dependent on peaks, simplest method
Edge-based	Discontinuity detection	Relevant for images having good contrast	Not suitable a large
Cluster-based	Homogeneous clusters	Use of membership function to address the real-life problems	The evaluating membership function is not an easy task
Region-based	Based on splitting image into consistent regions	More protective for noise	Expensive in terms of memory and time
PDE-based	Used differential equations	Fastest method	Computational complexity is higher than previous methods
Deep-learning based	Replication of learning process for decision making	Simple programs	Training data time is too high
Proposed Work	Finding the regions of interest (ROI) by capturing pixels with higher scores after activation to compute the membership functions T, I and F	This method can be applied to any number of images and any type of typical problem (blurred images)	No need to training, so it is less time consuming than deep learning approaches

Table 6
Comparison between the various types of image segmentation methods and our proposed model in terms of DS_{core} value.

Segmentation methods	Average D-score
Threshold based	0.56
Edge-based	0.62
Cluster-based	0.64
Region-based	0.67
PDE-based	0.70
Deep-learning based	0.73
Neutrosophic sets-based (Proposed work)	0.78

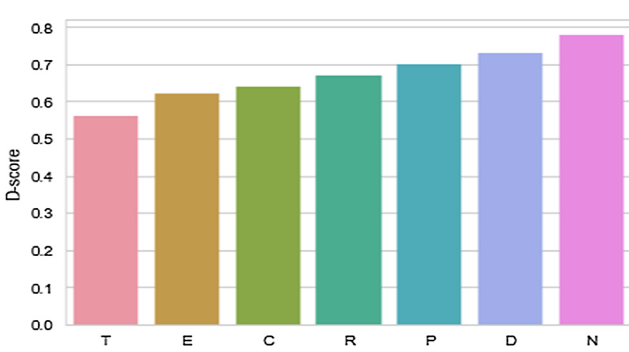

Fig. 9. Graphical representation of methods in terms of $DS_{core.}$

orientations only. The same is true for X-ray images as well. In these types of scenarios, Neutrosophic sets can be used effectively to analyze the problems. In the future, we can optimize this algorithm further to be applied to various other domains and surpass the current state-of-the-art deep neural networks.

Table 7
Comparison of the proposed work with existing ones.

No.	Authors	Existing methods	Proposed method
1.	Liang-Chieh Chen et al. [44]	- Used benchmarking of pre-release Cityscapes dataset - Performance is 63.1%	- We have used three orientations of sample crow images and the datasets were generated by ourselves (Section 4) - Performance is 78% as depicted in Table 7
2.	Ma et al. [13]	- Used a generalized interval of Neutrosophic set values (higher number of assumptions) - Aggregated the interval Neutrosophic linguistic information. - Performance is 71%	- Very less assumptions made in our paper, due to which the results are more absolute than their work - The model works on different types of scenarios as well, which makes it unique from them on Image Segmentation using Neutrosophic sets because priority has been given to each Neutrosophic Set values (pixels) generated - Performance is 78%
3.	Irfan Deli et al. [45]	- Define the concepts of cut sets of SVN-numbers - Applied to single valued trapezoidal neutrosophic numbers - Developed a ranking method by using the concept of values and ambiguities	- Our paper defines basic concepts of Neutrosophic Set theory and - Applicable in various membership functions and fitness functions - Applied to multiple sets of values - Multiple set of values experimented for different image orientations - No ambiguities - We concluded with the absolute performance value of 78%

5. Conclusion

This paper explores the idea of applying Neutrosophic sets to the domain of Image Segmentation. We firstly discussed various properties of Neutrosophic sets and then lay out to tackle the problem of image segmentation with fewer assumptions. To accomplish this, we first used Min-Max Normalization to reduce any uncertain noise in the image that may be caused due to a number of factors during image capturing. Then, we applied activation functions to account for non-linearities in the image. We then computed the membership functions on different regions and formed the Neutrosophic sets. These sets are then transformed and compared with other sets to find similarities and dissimilarities.

Throughout the entire paper, we used images of a crow and presented our findings. It is worth noting that Neutrosophic sets can be applied to datasets with missing data with different orientations. This calls for a better understanding of Neutrosophic systems and their further research on solving complex problems simply and replace the current state-of-the-art methodologies. Using Neutrosophic Sets and using Dice's Coefficients (D_{Score}), this paper has resolved earlier sophisticated methods and ensured the proper evaluation of the uncertainty of the missing data and their indeterminacy with various results to prove effectiveness for the image processing and segmentation.

The proposed work could be refined further in order to achieve better results. Several other parameters may be considered for the same:

1. Neutrosophic sets (NS) can be remarkably used along with neural networks to get in depth of various fields. Natural Language Processing, Image Captioning etc are few of them.
2. Digital Communication have used lots of research to reduce internal noise in an image. They have also used many filters apart from quantization and sampling to reduce the noise and errors in an image. However, the Neutrosophic Set theory can be extensively used to predict indeterminacy and normalize them using various membership functions.
3. NS can be used for noise detection and minimization using various factors, such as poor lighting, dust particles blockage, etc. by normalization.
4. In short, the NS concept is best suitable in working conditions, i.e., the real time problems. For example, in medical diagnosis, it is very important to reduce noise before we perform any Image Processing as it is impossible to find best. We used an existing method for reducing noise which has proved effective in X-ray images significantly high.

References

[1] L.A. Zadeh, Fuzzy sets, Inform. Control 8 (1965) 338–353.
[2] Z. Pawlak, Rough sets, Int. J. Inform. Comput. Sci. 11 (1982) 341–356.
[3] F. Smarandache, Neutrosophic set, a generalisation of the intuitionistic fuzzy sets, Int. J. Pure Appl. Math. 24 (2005) 287–297.
[4] D.A. Molodtsov, Soft set theory-first results, Comput. Mathemat. Appl. 37 (1999) 19–31.
[5] H. Wang, F. Smarandache, Y.Q. Zhang, R. Sunderraman, Interval Neutrosophic Sets and Logic: Theory and Applications in Computing, Hexis, Neutrosophic book series, 2005, No 5.
[6] S. Broumi, F. Smarandache, Correlation coefficient of interval neutrosophic set, in: Applied Mechanics and Materials, Trans Tech Publications, 2013, pp. 511–517.
[7] A.R. Solis, G. Panoutsos, Granular computing neural-fuzzy modelling: a neutrosophic approach, Appl. Soft Comput. 13 (9) (2013) 4010–4021.
[8] J. Ye, Multicriteria decision-making method using the correlation coefficient under single-valued neutrosophic environment, Int. J. Gen. Syst. 42 (4) (2013) 386–394.
[9] J. Ye, A multicriteria decision-making method using aggregation operators for simplified neutrosophic sets, J. Intell. Fuzzy Syst. 26 (5) (2014) 2459–2466.
[10] J. Ye, Vector similarity measures of simplified neutrosophic sets and their application in multicriteria decision making, Int. J. Fuzzy Syst. 16 (2) (2014).
[11] J.J. Peng, J.Q. Wang, H.Y. Zhang, X.H. Chen, An outranking approach for multi-criteria decision-making problems with simplified neutrosophic sets, Appl. Soft Comput. 25 (2014) 336–346.
[12] J.J. Peng, J.Q. Wang, X.H. Wu, J. Wang, X.H. Chen, Multi-valued neutrosophic sets and power aggregation operators with their applications in multi-criteria group decision-making problems, Int. J. Comput. Intell. Syst. 8 (2) (2015) 345–363.
[13] Y.X. Ma, J.Q. Wang, J. Wang, X.H. Wu, An interval neutrosophic linguistic multi-criteria group decision-making method and its application in selecting medical treatment options, Neural Comput. Appl. 28 (9) (2017) 2745–2765.
[14] I. Deli, Y. Şubaş, A ranking method of single valued neutrosophic numbers and its applications to multi-attribute decision making problems, Int. J. Machine Learn. Cybernet. 8 (4) (2017) 1309–1322.
[15] J. Ye, Improved cosine similarity measures of simplified neutrosophic sets for medical diagnoses, Artificial Intell. Med. 63 (3) (2015) 171–179.
[16] M. Abdel-Basset, M. Mohamed, The role of single valued neutrosophic sets and rough sets in smart city: imperfect and incomplete information systems, Measurement 124 (2018) 47–55.
[17] Y. Guo, A. Şengür, Y. Akbulut, A. Shipley, An effective color image segmentation approach using neutrosophic adaptive mean shift clustering, Measurement 119 (2018) 28–40.
[18] K.M. Amin, A.I. Shahin, Y. Guo, A novel breast tumor classification algorithm using neutrosophic score features, Measurement 81 (2016) 210–220.
[19] J. Ye, Single valued neutrosophic cross-entropy for multicriteria decision making problems, Appl. Mathemat. Modell. 38 (3) (2014) 1170–1175.
[20] J. Ye, Fault diagnoses of hydraulic turbine using the dimension root similarity measure of single-valued neutrosophic sets, Intell. Automat. Soft Comput. (2016).
[21] J. Ye, Single-valued neutrosophic similarity measures based on cotangent function and their application in the fault diagnosis of steam turbine, Soft Comput. 21 (3) (2017) 817–825.
[22] J. Ye, S. Du, Some distances, similarity and entropy measures for interval valued neutrosophic sets and their relationship, Int. J. Machine Learn. Cybernet. (2017), https://doi.org/10.1007/s13042-017-0719-z.
[23] M. Ali, H. Khan, L. Son, F. Smarandache, W. Kandasamy, New soft set based class of linear algebraic codes, Symmetry 10 (10) (2018) 510.
[24] S. Doss, A. Nayyar, G. Suseendran, S. Tanwar, A. Khanna, P.H. Thong, APD-JFAD: accurate prevention and detection of jelly fish attack in manet, IEEE Access 6 (2018) 56954–56965.
[25] A. Dey, L. Son, P. Kumar, G. Selvachandran, S. Quek, New concepts on vertex and edge coloring of simple vague graphs, Symmetry 10 (9) (2018) 373.
[26] L. Amal, L.H. Son, H. Chabchoub, SGA: spatial GIS-based genetic algorithm for route optimization of municipal solid waste collection, Environ. Sci. Pollut. Res. 25 (27) (2018) 27569–27582.
[27] L.H. Son, H. Fujita, Neural-fuzzy with representative sets for prediction of student performance, Appl. Intell. 1–16 (2018), https://doi.org/10.1007/s10489-018-1262-7.
[28] T. Le, H. Le Son, M. Vo, M. Lee, S. Baik, A Cluster-based boosting algorithm for bankruptcy prediction in a highly imbalanced dataset, Symmetry 10 (7) (2018) 250.
[29] L.H. Son, F. Chiclana, R. Kumar, M. Mittal, M. Khari, J.M. Chatterjee, S.W. Baik, ARM–AMO: an efficient association rule mining algorithm based on animal migration optimization, Knowledge-Based Syst. 154 (2018) 68–80.
[30] The meaning of three black crows, International trend and foreign exchange, http://highvpnrklw.tk/meaning-of-three-black-crows-971664.html.
[31] A. Taha, A. Hanbury, Metrics for evaluating 3D medical image segmentation: analysis, selection, and tool, BMC Med. Imag. (2015).
[32] D.H. Thai, S. Huckemann, C. Gottschlich, Filter design and performance evaluation for fingerprint image segmentation, PLoS ONE 11 (5) (2016), https://doi.org/10.1371/journal.pone.0154160 e0154160.
[33] A. Bose, K. Mali, Fuzzy-based artificial bee colony optimization for gray image segmentation, Signal Image Video Process. 32 (4) (2016) 87–96.
[34] H. Moftah, A. Azar, E. Shammari, N. Ghali, A. Hassanien, M. Shoman, Adaptive k-means clustering algorithm for MR breast image segmentation, Neural Comput. Appl. 51 (2) (2014) 147–156.
[35] Y. Liu, C. Mu, W. Kou, J. Liu, Modified particle swarm optimization-based multilevel thresholding for image segmentation, Soft Comput. 41 (1) (2014) 54–64.
[36] M. Ayyoub, A. Dalo, Y. Jararweh, M. Jarrah, M. Sad, GPU-based implementations of the fuzzy C-means algorithms for medical image segmentation, J. Supercomput. 52 (2) (2015) 89–95.
[37] M. Kloster, G. Kauer, B. Beszteri, SHERPA: an image segmentation and outline feature extraction tool for diatoms and other objects, BMC Bioinformatics 74 (5) (2014) 48–56.
[38] D. Chen, G. Li, Y. Sun, J. Kong, G. Jiang, H. Tang, Z. Ju, H. Yu, H. Liu, An Interactive Image Segmentation Method in Hand Gesture Recognition, School of Machinery and Automation, Wuhan University of Science and Technology, 2017, pp. 74–85.
[39] L. Yu, J. Xie, X. Chen, Semantic image segmentation method with multiple adjacency trees and multiscale features, Cognit. Comput. 47 (8) (2017) 39–45.
[40] Y. Guo, R. Xia, A. Sengur, K. Polat, A novel image segmentation approach based on neutrosophic c-means clustering and indeterminacy filtering, Neural Comput. Appl. 13 (5) (2017) 149–158.
[41] L.H. Son, T.M. Tuan, Dental segmentation from X-ray images using semi-supervised fuzzy clustering with spatial constraints, Eng. Appl. Artificial Intell. 59 (2017) 186–195.
[42] L. Nýul, Fuzzy techniques for image segmentation, Univer. Szeged 54 (5) (2008) 57–67.
[43] M. Badea, I. Felea, C. Vertan, L. Florea, The Use of Deep Learning in Image Segmentation Classification and Detection, Computer Vision and Pattern Recognition 62(5)2016, pp. 187–198.
[44] L. Chen et al. DeepLab: Semantic Image Segmentation with Deep Convolutional Nets, Atrous Convolution, and Fully Connected CRFs 2017 https://arxiv.org/abs/1606.00915.
[45] I. Deli, Y. Subas, A ranking method of single valued neutrosophic numbers and its applications to multi-attribute decision making problems, J. Mach. Learn. Cybernet. Int. (2017), https://doi.org/10.1007/s13042-016-0505-3.
[46] T.M. Tuan, T.T. Ngan, L.H. Son, A novel semi-supervised fuzzy clustering method based on interactive fuzzy satisficing for dental X-ray image segmentation, Appl. Intell. 45 (2) (2016) 402–428.
[47] S. Broumi et al., An introduction to bipolar single valued neutrosophic graph theory, Appl. Mech. Mater. 84 (1) (2016) 184–191.
[48] S. Broumi, Bipolar Neutrosophic Minimum Spanning Tree, Smart Application and Data Analysis for Smart Cities, 201–206, 2018. doi: 10.2139/ssrn.3127519
[49] A. Dey, A new algorithm for finding minimum spanning trees with undirected neutrosophic graphs, Granular Comput. 2018 (2018), https://doi.org/10.1007/s41066-018-0084-7.
[50] S. Broumi et al., A bipolar single valued neutrosophic isolated graphs: revisited, Int. J. New Comput. Architect. Their Appl. (IJNCAA) 7 (3) (2017) 89–94.
[51] S. Broumi et al., A matlab toolbox for interval valued neutrosophic matrices for computer applications, Uluslararası Yönetim Bilişim Sistemleri ve Bilgisayar Bilimleri Dergisi 1 (1) (2017) 1–21.
[52] S. Broumi et al., Computing minimum spanning tree in interval valued bipolar neutrosophic environment, Int. J. Model. Optimizat. 7 (5) (2017) 300–304, https://doi.org/10.7763/IJMO.2017.V7.602.
[53] S. Broumi et al. Computation of Shortest Path Problem in a Network with SV-Trapezoidal Neutrosophic Numbers, Proceedings of the 2016 International

Conference on Advanced Mechatronic Systems, Melbourne, Australia, pp. 417–422.
[54] S. Broumi et al. Applying Dijkstra Algorithm for Solving Neutrosophic Shortest Path Problem, Proceedings of the 2016 International Conference on Advanced Mechatronic Systems, Melbourne, Australia, pp. 412-416.
[55] T.M. Tuan, P.M. Chuan, M. Ali, T.T. Ngan, M. Mittal, L.H. Son, Fuzzy and neutrosophic modeling for link prediction in social networks, Evolv. Syst. 1–6 (2018), https://doi.org/10.1007/s12530-018-9251-y.
[56] M. Khan, L. Son, M. Ali, H. Chau, N. Na, F. Smarandache, Systematic review of decision making algorithms in extended neutrosophic sets, Symmetry 10 (8) (2018) 314.
[57] S. Jha, R. Kumar, L.H. Son, J.M. Chatterjee, M. Khari, N. Yadav, F. Smarandache, Neutrosophic soft set decision making for stock trending analysis, Evolv. Syst. 1–7 (2018), https://doi.org/10.1007/s12530-018-9247-7.
[58] A. Dey, S. Broumi, L.H. Son, A. Bakali, M. Talea, F. Smarandache, A new algorithm for finding minimum spanning trees with undirected neutrosophic graphs, Granular Comput. 1–7 (2018), https://doi.org/10.1007/s41066-018-0084-7.
[59] M. Ali, L.H. Son, N.D. Thanh, N. Van Minh, A neutrosophic recommender system for medical diagnosis based on algebraic neutrosophic measures, Appl. Soft Comput. 71 (2018) 1054–1071.
[60] G.N. Nguyen, L.H. Son, A.S. Ashour, N. Dey, A survey of the state-of-the-arts on neutrosophic sets in biomedical diagnoses, Int. J. Mach. Learn. Cybernet. 1–13 (2018), https://doi.org/10.1007/s13042-017-0691-7.
[61] S. Broumi, L.H. Son, A. Bakali, M. Talea, F. Smarandache, G. Selvachandran, Computing operational matrices in neutrosophic environments: A Matlab Toolbox, Neutrosophic Sets Syst. 18 (2017).
[62] S. Broumi, A. Dey, A. Bakali, M. Talea, F. Smarandache, L.H. Son, D. Koley, Uniform single valued neutrosophic graphs, Neutrosophic Sets Syst. 17 (2017) 42–49.
[63] M. Ali, L.H. Son, I. Deli, N.D. Tien, Bipolar neutrosophic soft sets and applications in decision making, J. Intell. Fuzzy Syst. 33 (6) (2017) 4077–4087.
[64] N.X. Thao, B.C. Cuong, M. Ali, L.H. Lan, Fuzzy Equivalence on Standard and Rough Neutrosophic Sets and Applications to Clustering Analysis, in: In Information Systems Design and Intelligent Applications, Springer, Singapore, 2018, pp. 834–842.
[65] N.D. Thanh, M. Ali, A novel clustering algorithm in a neutrosophic recommender system for medical diagnosis, Cognit. Comput. 9 (4) (2017) 526–544.
[66] N.D. Thanh, L.H. Son, M. Ali, Neutrosophic recommender system for medical diagnosis based on algebraic similarity measure and clustering, in: In Fuzzy Systems (FUZZ-IEEE), 2017 IEEE International Conference on, IEEE, 2017, pp. 1–6.
[67] L.H. Son, T.M. Tuan, A cooperative semi-supervised fuzzy clustering framework for dental X-ray image segmentation, Expert Syst. Appl. 46 (2016) 380–393.